Title

18 Structural health monitoring strategy for damage detection in railway bridges using traffic induced dynamic responses

Authors

Meixedo, Andreia
Ribeiro, Diogo
Santos, João
et al.

Publication Date

2022

DOI

10.1016/b978-0-12-821042-0.00011-3

Peer reviewed

Structural health monitoring strategy for damage detection in railway bridges using traffic induced dynamic responses

18

Andreia Meixedo[a], Diogo Ribeiro[b], João Santos[c], Rui Calçada[a], and Michael Todd[d]
[a]CONSTRUCT—LESE, Faculty of Engineering (FEUP), University of Porto, Porto, Portugal, [b]CONSTRUCT-LESE, School of Engineering, Polytechnic of Porto, Porto, Portugal, [c]LNEC, National Laboratory for Civil Engineering, Lisbon, Portugal, [d]Department of Structural Engineering, University California San Diego, San Diego, CA, United States

18.1 Introduction

The high dependency of modern societies on structural and mechanical systems leads to an active field of research that aims to reduce the costs of visual inspection and maintenance. Particularly, the maintenance of bridges is central to the structural integrity and cost-effectiveness of any transportation system [1]. However, in the case of railway infrastructures, their intense use by frequent and heavy traffic makes the task of detection and possible repair of damaged sections problematic. Moreover, many of these infrastructures are currently nearing the end of their life cycle.

Because these systems cannot be economically replaced, techniques for damage detection that make use of structural monitoring in real-time, are being developed and implemented so that these infrastructures can continue to be safely used if their operation is extended beyond the design basis service life. These circumstances demand that the onset of damage in new systems can be detected at the earliest possible time to prevent failures that can have serious life safety and economic consequences [2].

Structural Health Monitoring (SHM) represents a promising strategy in this ongoing challenge to achieve sustainable infrastructure since it has the potential to identify a structural change before it becomes critical. SHM for damage detection involves the collection of reliable data on the baseline condition of a bridge, the observation of its evolution over time, and the characterization of the degradation. By permanently installing a number and variety of sensors, which continuously measure structural responses, it is possible to obtain a real-time representation of the structure's current state. However, this information is only useful by assuring that reliable SHM systems, methods for data analysis, and statistics tools are put into practice.

In this context, the present research work aims at developing and validating an SHM strategy for damage detection in railway bridges using traffic-induced

Rail Infrastructure Resilience. https://doi.org/10.1016/B978-0-12-821042-0.00011-3

dynamic responses. To achieve this goal, an unsupervised data-driven strategy is implemented, consisting of multivariate statistical techniques. The signals resulting from train crossings correspond to a large mass traveling at significant speeds, thus generating features that can obscure information associated with damage. The set of techniques implemented herein allows removing all the train-related features to expose, with high sensitivity, those generated by damage. The effectiveness of the proposed methodology is validated in a long-span steel-concrete composite bowstring arch railway bridge tuned with a permanent structural monitoring system. An experimentally validated finite element model was used, along with experimental values of temperature, noise, and train loadings and speeds, to realistically simulate baseline and damage scenarios.

After this introduction, in Section 18.2, a literature review on SHM for damage detection is conducted. Section 18.3 presents the case study, detailing the monitoring system installed and the simulation of different structural conditions. In Section 18.4, the strategy for damage detection is implemented and validated. Finally, Section 18.5 presents the main conclusions drawn from this research work.

18.2 Literature review on SHM for damage detection

The assessment of damage usually requires a comparison between two states and, consequently, each SHM approach requires a baseline system. How the training set is defined will depend on which level of damage detection is aimed and, therefore, the data set can be established based on normal conditions only or a combination of normal and damaged conditions of the structure. Hence, SHM for damage detection can be seen as a four-step process (Fig. 18.1): (i) operational evaluation, (ii) data acquisition, (iii) feature extraction and (iv) feature discrimination.

The first step to developing an SHM strategy is to perform an operational evaluation. This phase attempts to provide answers to four questions, which are mentioned in Fig. 18.1, regarding the implementation of a damage detection investigation [3,4]. By providing answers to these questions, the operational evaluation process begins to set limitations on what will be monitored and how the monitoring will be accomplished.

Obtaining accurate measurements of a system's dynamic response is essential to SHM. There are many different sensors and data acquisition systems that can be applied to the SHM problem and the one employed will be application-specific. In this sense, Fig. 18.1 details the several considerations that one should make during the data acquisition step.

Identifying features that can accurately distinguish a damaged structure from an undamaged one is the focus of most SHM technical literature. Fig. 18.1 summarizes the main ideas that support the third step of the process, i.e., the feature extraction.

Fundamentally, feature extraction refers to the process of transforming the measured data into some alternative form where the correlation with the damage is more readily observed [5]. Often in SHM, the feature extraction process is based on fitting some model, either physics-based or data-based, to the measured response data. The parameters of these models, quantities derived from the parameters, or the

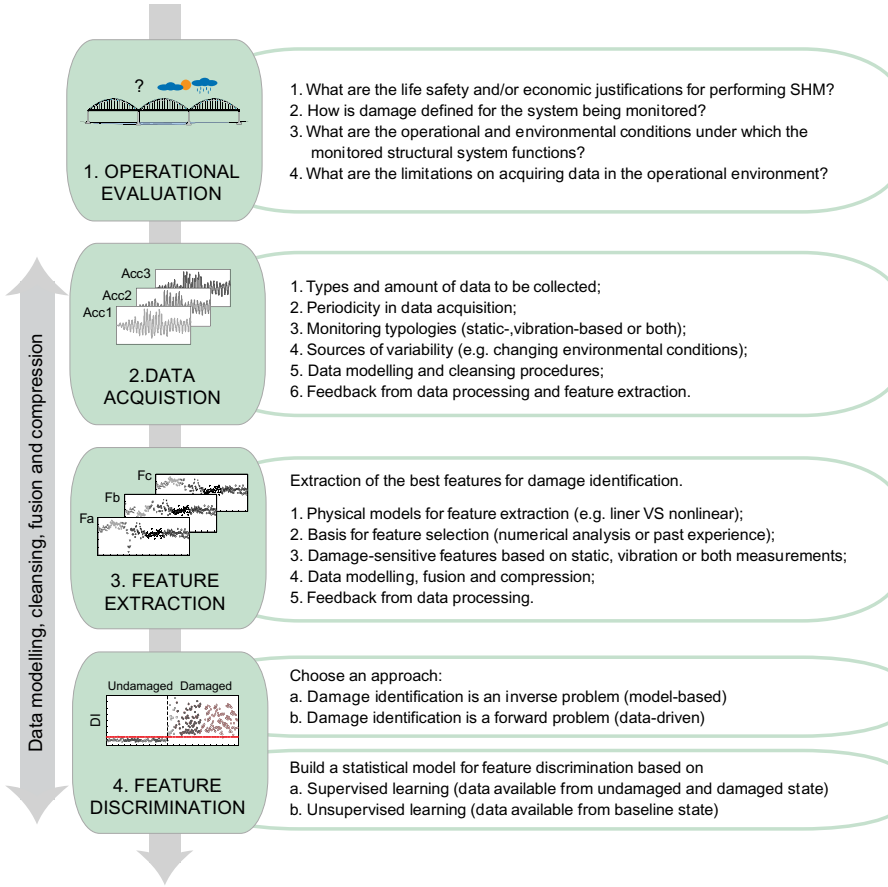

Fig. 18.1 SHM for damage detection as a four-step process.

predictive errors associated with these models, become then the damage-sensitive features [6].

Modal or model-based features are the most common in the literature [7–11] due to the advantage of being directly associated with the mass and, more importantly, with structural stiffness, which is expected to change in the presence of damage. Regardless of these advantages, OMA-based information can also be considered not sensitive to early damage due to the need of identifying high order modes shapes, which proved to be very challenging for real structure monitoring [12]. Symbolic data [13], wavelet components [14] and basic signal statistics are also examples of techniques successfully applied as extractors of damage-sensitive features for both static and dynamic monitoring. In applications comprising acceleration measurements, autoregressive (AR) models, wavelets, and principal component analysis (PCA) have been widely reported [12,15–21].

Once an operational evaluation stage has passed and a sensor network has been designed, the SHM system can begin to deliver data. At this stage, one is now faced with the challenge of making an accurate assessment of the damage condition of a given structure based on any extracted features. Feature discrimination, which comprises the choice and implementation of algorithms to process the data and carry out the identification, is arguably the most crucial component of an intelligent SHM strategy for damage detection. Before even choosing the algorithm, it is necessary to choose between two complementary approaches to the problem, as described in Fig. 18.1: (a) model-based or (b) data-driven.

The inverse approach (model-based) combines an initial model of the structure and measured data to improve the model or test a hypothesis. In practice, the model is commonly based on finite element analysis. Once the model is built, it is updated based on measured data from the real structure, such as acceleration and force responses, often in the form of a modal database, although frequency response function data may also be directly used [22,23]. The goal is to adjust the built model in such a way as to make it conform better with data from the real structure. Although, it is important to be aware that the updating step brings up an important point; it is very difficult to build an accurate model of a structure since the information will be lacking in many areas. For example, the material properties may not be known with great accuracy, especially in civil engineering where each structure is unique.

In turn, the forward approach (data-driven) does not require the development of numerical or analytical models to be fitted with in situ data; instead, it is based on the discipline of machine learning or, often more specifically, the pattern recognition aspects of machine learning. The idea is that one can learn relationships from data. In the context of SHM, this means that one can learn to assign a damage state or class to a given measurement vector from the structure or system of interest. The measurement vectors must be formed from measurements that are sensitive to the damage; in the normal terminology of pattern recognition, they are referred to as features, as previously discussed. Once features have been defined, the mapping between the features and the diagnosis can be constructed. In the forward approach, one can still make effective use of the law-based models as a means of establishing good features for damage identification [24].

The portion of the SHM process that is less documented in the technical literature is the development of statistical models for discrimination between features from the undamaged and damaged structures. Statistical model development is concerned with the implementation of algorithms that operate on the extracted features to quantify the damage state of the structure. The functional relationship between the selected features and the damage state of the structure is often difficult to define. Therefore, the statistical models are derived using machine learning techniques. The machine learning algorithms used in statistical model development for feature discrimination usually fall into two categories (i) supervised learning and (ii) unsupervised learning, see Fig. 18.1.

When training data is available from both undamaged and damaged structures, supervised learning algorithms can be used; group classification and regression analysis are primary examples of such algorithms. In the case of group classification, the

output of the algorithm is a discrete class label. In its most basic form, this algorithm might simply assign a "damage" or "not damage" label to features. This type of algorithm is useful in the sense that the algorithms can be trained to give the probability of class membership. Using a regression algorithm, the outputs are one or more continuous variables. This problem is often nonlinear and is particularly suited to neural networks or other machine learning algorithms [3].

Since data obtained from damaged civil engineering structures is rare or inexistent, unsupervised learning algorithms have been increasingly observed in the literature. Damage detection methods are the primary class of algorithms used in this situation. This type of algorithm is a two-class problem that indicates if the acquired data comes from normal operating conditions or not [3]. There are many damage detection techniques, e.g., outlier analysis, kernel density estimation, and auto-associative neural networks [25,26]. All techniques fit a probability distribution to the normal condition data, then assess the probability of the test data having been generated by the same mechanism. It is important to notice that supervised and unsupervised learning come usually associated with a forward damage identification approach.

Inherent in the data acquisition, feature extraction, and feature discrimination portions of the SHM strategy are data cleansing, fusion, and compression procedures, as well as data modeling (see Fig. 18.1). Data cleansing is the process of selectively choosing data to pass on to, or reject from, the feature selection process. On the other hand, data fusion focuses on reducing the volume of data, while preserving its most relevant information. The fusion process may combine features from a single sensor, features from spatially distributed sensors, or even heterogeneous data types. In all situations, the objective of a data fusion process is to reach a new type of information with less volume and greater or similar ability to characterize the measured phenomena, when compared to that achieved when using any of the original information sources alone [27]. The Mahalanobis distance has been thoroughly used in this context due to its capacity to describe the variability in multivariate data sets [7,28]. Data compression, in turn, is the process of reducing the dimensionality of the data, or the features extracted from the data, to facilitate efficient storage of information and to enhance the statistical quantification of these parameters.

The ability to perform robust data modeling is one of the biggest challenges facing SHM when attempting to transition this technology from research to field deployment and practice on in situ structures [2]. As it applies to SHM, data modeling is the process of separating changes in sensor reading caused by damage from those caused by varying operational and environmental conditions, such as temperature or trains crossing at different speeds [29]. Two approaches are generally found in the literature and in the practice of feature modeling [12]: (i) input-output, based on regression methods such as multiple linear regression (MLR) [30,31] or (ii) output-only, based on latent variable methods such as PCA [8,12]. The first removes the effects of the environmental and operational variations (EOVs), establishing relationships between measured actions (e.g., temperature, traffic, wind) and measured structural responses. When monitoring systems do not include the measurement of EOVs, latent variable methods can be employed. These methods are able to suppress independent actions using only structural measurements.

18.3 Railway bridge over the Sado River

18.3.1 Bridge description

A bowstring-arch railway bridge over the Sado River was selected as the case study used throughout this work. It is located on the southern line of the Portuguese railway network that establishes the connection between Lisbon and the Algarve (Fig. 18.2). The bridge is prepared for conventional and tilting passenger trains with speeds up to 250 km/h, as well as for freight trains with a maximum axle load of 25 t. Even though the bridge accommodates two rail tracks, only the upstream track is currently in operation.

The bridge has a total length of 480 m, divided into three continuous spans of 160 m each. The bridge deck is suspended by three arches connected to each span of the deck by 18 hangers distributed over a single plane on the axis of the structure. The superstructure is composed of a steel-concrete composite deck, while the substructure, which includes the piers, the abutments, and the pile foundations, is built with reinforced concrete. The deck is fixed on pier P1, whereas on piers P2, P3, and P4 only the transverse movements of the deck are restrained, while the longitudinal movements are constrained by seismic dampers.

18.3.2 Monitoring system

The structural health condition of the railway bridge over the Sado River has been controlled with a comprehensive autonomous online monitoring system, as detailed in Fig. 18.3, since the beginning of its life cycle. This monitoring system was defined based on an operational evaluation and allowed the acquisition of data necessary to implement the strategy for damage detection (steps 1 and 2 of Fig. 18.1).

To identify each train that crosses the bridge and compute its speed, two pairs of optical sensors were installed at both ends of the bridge. The structural temperature

Fig. 18.2 Overview of the bridge over the Sado River.

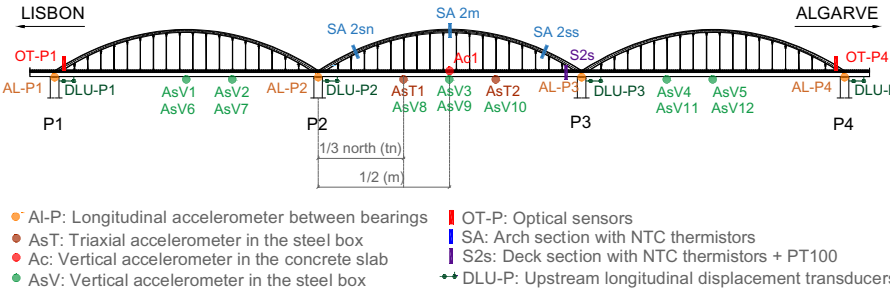

Fig. 18.3 The SHM system of the railway bridge over the Sado River.

action is measured using PT100 thermometers and NTC thermistors. Three sections of the arch were instrumented with 12 NTC thermistors. Additionally, four NTC thermistors were fixed to the steel box girder and three PT100 thermometers were embedded in the concrete slab. To control the behavior of the bearing devices, the responses from longitudinal displacement transducers were obtained from four sensors, each adjacent to a bearing device. The set of sensors also includes one vertical piezoelectric accelerometer fixed at the midspan of the concrete slab, two triaxial force balance accelerometers at the thirds of the midspan steel box girder, and 12 vertical force balance accelerometers fixed along each span of the steel box girder. Four longitudinal MEMS DC accelerometers were also installed at the top of each pier. Data acquisition is carried out continuously, at a sampling rate of 2000 Hz, by a locally deployed industrial computer to save the time history during the passage of the trains.

18.3.3 Numerical modeling and validation

A simulation of healthy and damage scenarios was conducted to test and validate the strategy implemented in Section 18.4 since damage scenarios were not observed experimentally during the period of this research. After an effective validation of the strategy, it can be applied straight to experimental data from different types of bridges.

For this purpose, a 3D finite element (FE) numerical model of the bridge was developed in ANSYS software and fully validated with experimental data (Fig. 18.4A). Among the modeled structural elements, those defined as beam finite elements consist of piers, sleepers, ballast-containing beams, rails, arches, hangers, transverse stiffeners, diaphragms, and diagonals. Shell elements were used to model the concrete slab and the steel box girder, while the pads, the ballast layer, and the foundations were modeled using linear spring-dashpot assemblies. The mass of the nonstructural elements and the ballast layer was distributed along with the concrete slab. Concentrated mass elements were used to reproduce the mass of the arches' diaphragms and the mass of the sleepers, which were simply positioned at their extremities. The connection between the concrete slab and the upper flanges of the steel box girder, as well as the connection between the deck and the track, were performed using rigid links. Special attention was paid to the bearings supports, as they can strongly influence the

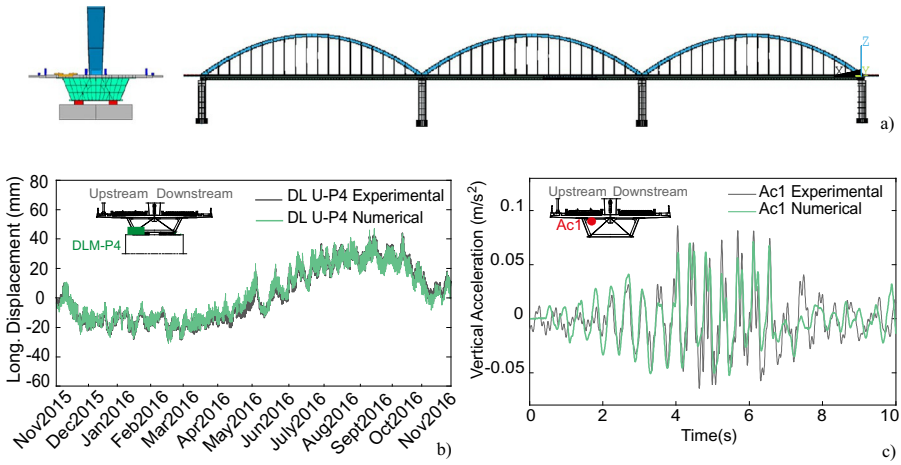

Fig. 18.4 Numerical modeling and validation: (A) 3D FE numerical model of the bridge over the Sado River, (B) static validation of the displacements measured on pier P4, and (C) dynamic validation of vertical accelerations at the concrete slab (Ac1) with the AP at 216 km/h.

performance of the bridge. Hence, to simulate the sliding behavior of the bearings, nonlinear contact elements were applied. Moreover, constraint elements located between the bearings were used to restrict the transversal movement in each pier, and the longitudinal and transversal movements in the case of the first pier.

To validate the static behavior of the numerical model, the response of the structure to the action of temperature was studied. The structural static behavior of the bridge was simulated in the FE model by running a time-history analysis using experimental data as input. The simulation procedure consisted of using the temperatures acquired every hour on-site over the course of 1 year. Fig. 18.4B presents a very good agreement between the numerical and experimental displacements of pier P4 for the temperature measured on-site between November 2015 and November 2016.

Regarding the dynamic behavior, numerical simulations were conducted considering the Alfa Pendular (AP) train as a set of moving loads crossing the bridge over the Sado River at a speed of 216 km/h. Fig. 18.4C shows a very good agreement between the experimental and numerical responses, in terms of the vertical accelerations acquired on the concrete slab at the second midspan (Ac1). Before the comparison, the time series were filtered based on a low-pass digital filter with a cut-off frequency equal to 15 Hz.

A detailed description of the numerical model and its validation can be found in Meixedo et al. [32].

18.3.4 Simulation of different structural conditions

The dynamic numerical simulations implemented in the present research work aimed at replicating the structural quantities measured in the exact locations of the accelerometers installed on-site (Fig. 18.3) during the passage of a train in the bridge.

To correctly reproduce these structural responses, the temperature action was introduced as input in the numerical model. The measurements of the optical sensors' setup were used to obtain the train speed and axle configuration, as well as the type of train.

The dynamic analyses mentioned hereafter were carried out for two of the passenger trains that typically cross the bridge over the Sado River, namely, the AP train and the Intercity (IC) train. Their frequent speeds on the bridge are 220 km/h for the AP train and 190 km/h for the IC train. The nonlinear problem was solved based on the Full Newton-Raphson method and the dynamic analyses were performed by the Newmark direct integration method, using a methodology of moving loads [9]. The integration time step (Δt) used in the analyses was 0.005 s.

Fig. 18.5A summarizes the 100 simulations of the baseline (undamaged) condition that aim at reproducing the responses of the bridge taking into account the variability of temperature, speed, type of train, and loading schemes (LS) [33].

On the other hand, the damage scenarios were chosen based on possible vulnerabilities identified for the type of structural system, taking into account its materials, behavior, loadings, and connections [34]. As shown in Fig. 18.5B, damage scenarios were simulated according to different groups:

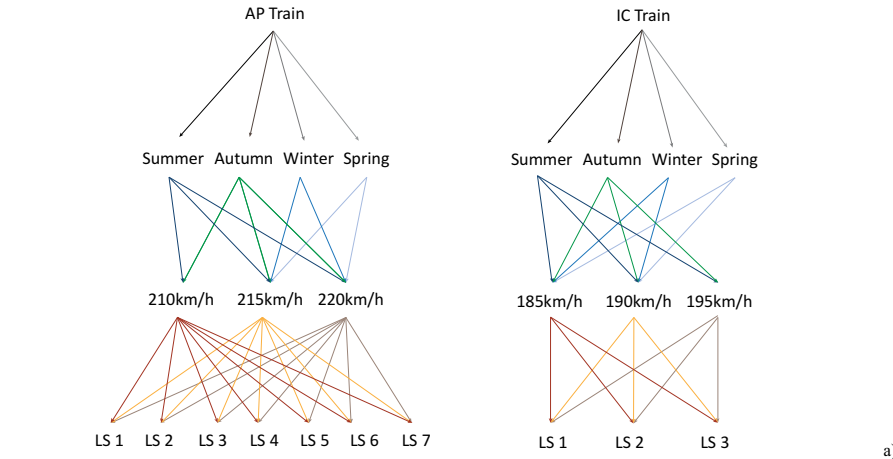

Fig. 18.5 Baseline and damage scenarios: (A) combination of 100 simulations for the baseline condition, (B) types of damages and their location on the bridge over the Sado River.

(i) damage in the bearing devices (type D1);
(ii) damage in the concrete slab (type D2);
(iii) damage in the diaphragms (type D3);
(iv) damage in the arches (type D4).

Each scenario was simulated considering only one damage location. Regarding the group of type D1, four severities of damage were included, namely, increases of the friction coefficient from a reference value of 1.5% to 1.8%, 2.4%, 3.0%, as well as to a full restrain of the movements between the pier and the deck. The remaining damage scenarios consisted of 5%, 10%, and 20% stiffness reductions in the chosen sections of the bridge (Fig. 18.5B) on the concrete slab (type D2), the diaphragms (type D3), and arches (type D4). These structural changes were simulated by reducing the modulus of elasticity of concrete (type D2) and of steel (types D3 and D4). A total of 114 damage scenarios were simulated for AP train crossings.

To obtain the most reliable reproduction of the real SHM data, the noise measured on-site by each accelerometer was added to the corresponding numerical output. These noise distributions were acquired while no trains were traveling over the bridge and under different ambient conditions. Each simulation was corrupted with different noise signals acquired at different days, thus ensuring the most representative validation for the techniques developed herein.

The time-series illustrated in Fig. 18.6 are examples of simulated responses for baseline and damage conditions, acquired from the accelerometer Ac1.

The variations associated with different train types, loading schemes, and train speeds are shown in Fig. 18.6A1 and A2. A clear distinction between the bridge responses for the IC (Fig. 18.6A1) train and the AP train (Fig. 18.6A2) passages can be observed, thus displaying the necessity of taking into account different train types for implementing damage detection strategies. Contrariwise, Fig. 18.6A1 allows observing that different LS generate smaller changes in the dynamic responses. The train speed also has an important influence on the structural response induced by trains crossing the bridge, as shown in Fig. 18.6A2.

The influence of damage scenarios in the signal obtained for the train crossings appears to be much smaller than that observed for changes in operational and environmental conditions, even when regarding sensors adjacent to the damages and for the biggest magnitudes considered (20% stiffness reductions). This conclusion can be easily observed in Fig. 18.6B1 and B2, where the bridge responses considering friction increments in the bearing devices of pier P2 and stiffness reductions in the concrete slab are, respectively, presented.

18.4 Strategy for damage detection using train induced dynamic responses

18.4.1 Overview

To address steps 3 and 4 of Fig. 18.1, an unsupervised data-driven strategy for damage detection in bridges, based on traffic-induced dynamic responses, which aims at being as effective as robust, is presented in Fig. 18.7, and comprises the following main operations:

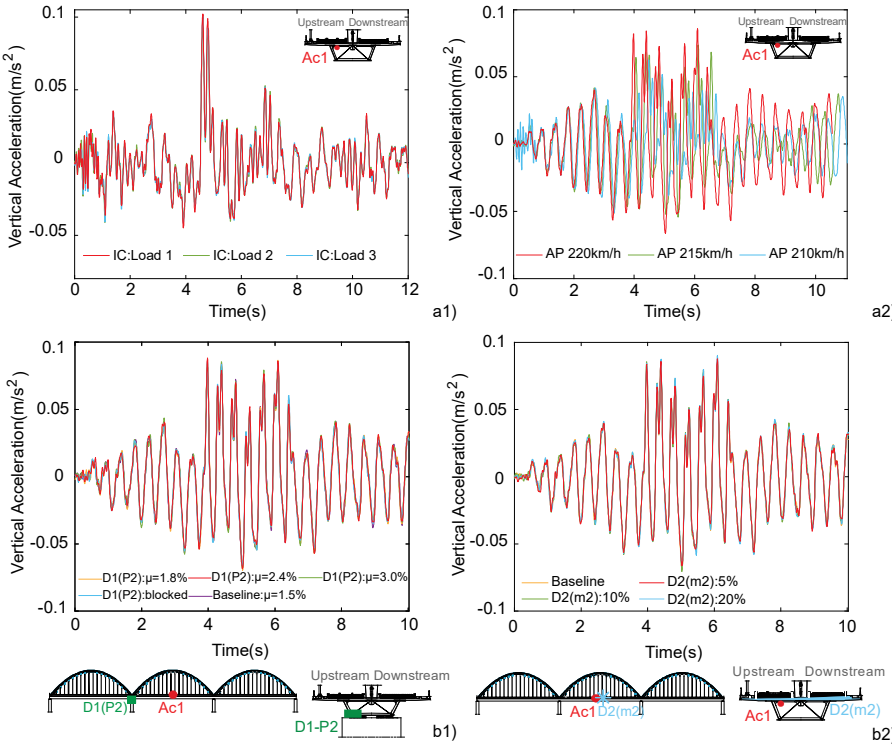

Fig. 18.6 Numerical simulations of sensor Ac1: (A1) baseline time-series using different LS of the IC train at 190 km/h, (A2) baseline time-series using different speeds of the AP train with LS5, (B1) damage time-series considering friction increase D1 (P2), and (B2) damage time-series considering stiffness reduction D2 (m2).

(i) damage-sensitive feature extraction from the acquired structural responses and feature modeling to remove EOVs, through the implementation of a double PCA (a latent-variable method);
(ii) data fusion using the Mahalanobis distance to merge multisensor features without losing damage related information;
(iii) feature discrimination to classify the extracted features in two categories, healthy or damaged, by applying an outlier analysis.

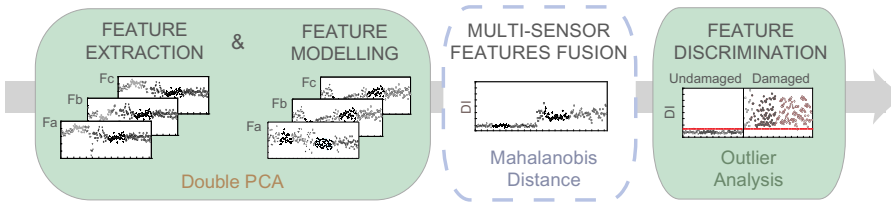

Fig. 18.7 Flowchart of the SHM strategy for damage detection.

18.4.2 Feature extraction and modeling—Double PCA

Feature extraction and feature modeling are addressed in this research work by implementing a double PCA. PCA is a multivariate statistical method that produces a set of linearly uncorrelated vectors called principal components, from a multivariate set of vector data [35].

The first operation intends to extract damage-sensitive features from the dynamic responses of the bridge. Considering an *n-by-m* matrix X with the original time series, where n is the number of measurements (i.e., 2112 in this case study) and m is the number of sensors (i.e., 23), a transformation to another set of m sensors, Y, designated principal components or scores, can be achieved by the following equation:

$$Y = X \cdot T \tag{18.1}$$

where T is an *m-by-m* orthonormal linear transformation matrix that applies a rotation to the original coordinate system. The covariance matrix of the measurements, C, is related to the covariance matrix of the scores, Λ, as follows:

$$C = T \cdot \Lambda \cdot T^T \tag{18.2}$$

in which T and Λ are matrixes obtained by the singular value decomposition of the covariance matrix C. The columns of T are the eigenvectors and the diagonal matrix Λ comprises the eigenvalues of the matrix C in descending order. Hence, the eigenvalues stored in Λ are the variances of the components of Y and express the relative importance of each principal component in the entire data set variation [7].

To allow data compression, four statistical parameters, namely the root mean square (RMS), the standard deviation, the Skewness, and the Kurtosis, are afterward extracted from the scores, Y. Thereby, the information presented in a matrix of *2112-by-23* is transformed into a matrix of *4-by-23*. A total of 92 features are thus extracted from the 23 acceleration measurements. This operation is implemented for each of the 214 structural conditions.

To illustrate the feature extraction procedure, the four statistical parameters obtained for two of the twenty-three sensors, AL-P1 and AsV3, are represented in Fig. 18.8. The eight features are divided according to the structural condition in two main groups: baseline (first 100 simulations) and damage (subsequent 114 simulations). A comparison between the values of the four features from each sensor, across all 214 scenarios, allows concluding that each statistical parameter is describing distinct trends in the analyzed data. Also, the information obtained from each feature is different depending on the sensor location. The main changes in the amplitudes of the features are induced by the type and speed of the trains. In addition, for each speed value, the changes observed in the amplitude of the statistical parameters are generated by changes in the structural temperature values (chosen for autumn, spring, summer, or winter). The different LS (the seven symbols in a row in the case of the AP and three symbols in a row in the case of the IC) considered for each train type and speed, and each temperature, are the operational factors with the smallest influence on the feature variability regarding the baseline simulations.

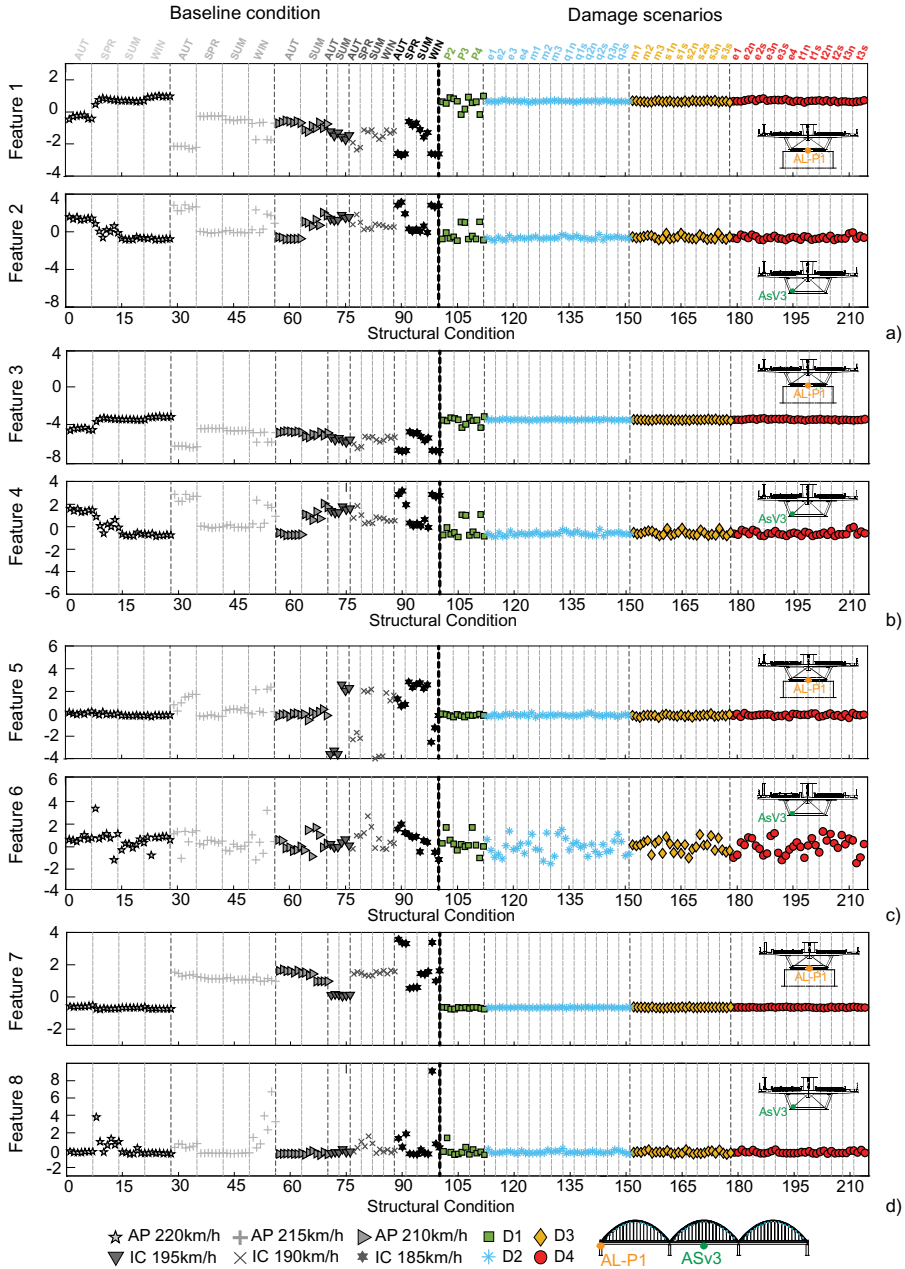

Fig. 18.8 Feature extraction of the responses from sensors AL-P1 and AsV3 for all 214 structural conditions: (A) RMS of the PCs, (B) standard deviation of the PCs, (C) Skewness of the PCs, and (D) Kurtosis of the PCs.

The analysis of the features shown in Fig. 18.8, as well as the time series presented in Fig. 18.6, allow drawing some conclusions about the difficulty in distinguishing undamaged and damage scenarios since the variations caused by environmental and operational effects result in similar or greater changes in the parameters.

Assuming that environmental conditions have a linear effect on the identified features, the implementation of a double PCA to the continuous monitoring results may efficiently remove environmental and operational effects, without the need to measure these actions [7,28].

Considering now an *n-by-m* matrix X with the features extracted from the dynamic responses, where n is the number of simulations for the baseline condition (i.e., 100 in this case study) and m is the number of features from all the sensors (i.e., 92), a transformation to another set of m parameters, Y, can be achieved by applying Eq. (18.1).

As demonstrated by Santos et al. [12], the PCA is able to cluster meaningful information related to EOVs in the first components, while variations related to other small-magnitude effects, such as early damage, may be retained in latter components. Since the purpose of the present research work is to detect damage, which has generally a local character, the feature modeling operation consists of eliminating the most important principal components (PCs) from the features and retaining the rest for subsequent statistical analysis. Bearing this in mind, the matrix Λ from Eq. (18.2) can be divided into a matrix with the first e eigenvalues and a matrix with the remaining m-e eigenvalues. Defining the number of e components remains an open question with regard to the representation of the multivariate data; although several approaches have been proposed, there is still no definitive answer [36]. In this work, the value of e (or the number of PCs to discard) is determined based on a rule of thumb in which the cumulative percentage of the variance reaches 80% [36,37]. After choosing e, the m-e components of the matrix Y can be calculated using Eq. (18.1) and a transformation matrix $\widehat{T}$ built with the remaining m-e columns of T. Those m-e components can be remapped to the original space using the following:

$$F_{\mathrm{PCA}} = X \cdot \widehat{T} \cdot \widehat{T}^{T} \tag{18.3}$$

where F_{PCA} is the *n-by-m* matrix of double PCA-based features, expected to be less sensitive to environmental and operational actions and to be more sensitive to the damage scenarios.

Since the cumulative percentage of the variance of the sum of the first six principal components was higher than 80% for different structural conditions, these six PCs were discarded during the modeling process (i.e., $e = 6$).

Fig. 18.9 shows the series of eight features across the 214 scenarios obtained for the AL-P1 and AsV3 accelerometers, after the application of the double PCA. The direct comparison of these action-free damage-sensitive features with those shown before the feature modeling (Fig. 18.8) allows observing that the feature modeling enabled removing the variations generated by the temperature, as well as by the type and speed of the train, but not those generated by damage. Moreover, the feature's sensitivity to the damage scenarios was increased.

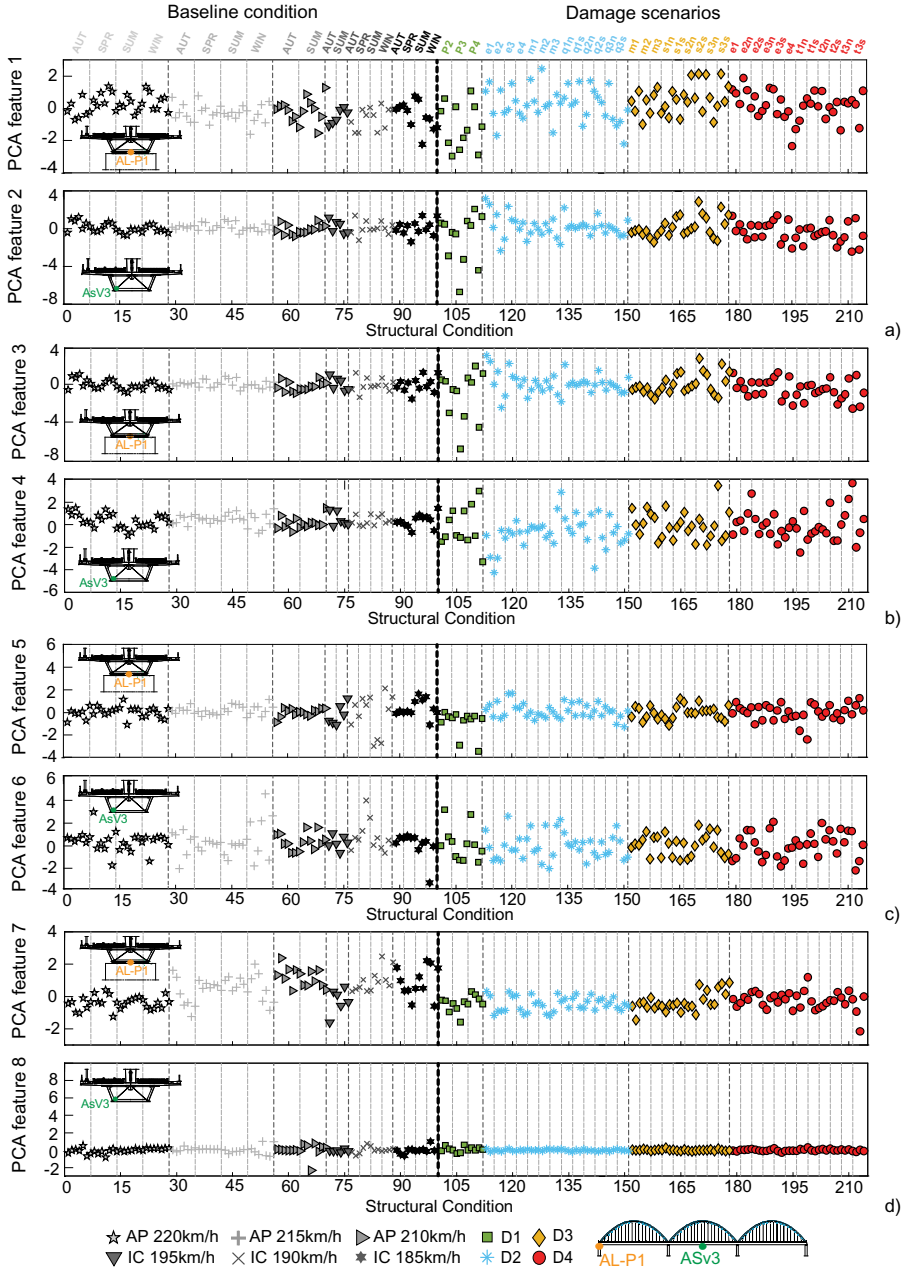

Fig. 18.9 Feature modeling of the features from sensors AL-P1 and AsV3 for all 214 structural conditions: (A) PCA of the RMS-based features, (B) PCA of the standard deviation-based features, (C) PCA of the Skewness-based features, and (D) PCA of the Kurtosis-based features.

18.4.3 Multisensor features fusion

To improve the features' discrimination sensitivity, data fusion was performed. A Mahalanobis distance was implemented to the modeled features, allowing for an effective fusion of the multisensor information. The outcome was a damage indicator, *DI*, for each train crossing. The analytical expression of the Mahalanobis distance for each simulation i, denoted as DI_i, is the following

$$DI_i = \sqrt{(x_i - \overline{x}) \cdot S_x^{-1} \cdot (x_i - \overline{x})^T} \tag{18.4}$$

where x_i is a vector of m features representing the potential damage/outlier, $\overline{x}$ is the matrix of the means of the features estimated in the baseline simulations, and S_x is the covariance matrix of the baseline simulations.

Hence, to detect all damage scenarios, a data fusion of the double PCA-based features from all the 23 sensors located on the bridge was implemented. It leads to a single vector *214-by-1* that represents all the data acquired through the 23 sensors. As a result, a clear distinction between simulations of the baseline condition and damage scenarios was achieved, as presented in Fig. 18.10.

18.4.4 Feature discrimination—Outlier analysis

Feature discrimination is addressed herein applying an outlier analysis that allows for automatic classification of each *DI* into healthy or damaged. A statistical confidence boundary *CB* based on the Gaussian inverse cumulative distribution (ICDF) function considering a mean μ and standard deviation σ of the baseline feature vector, and for a level of significance α is implemented. The inverse function can be defined in terms of the Gaussian cumulative distribution function as follows

$$CB = invF(1 - \alpha) \tag{18.5}$$

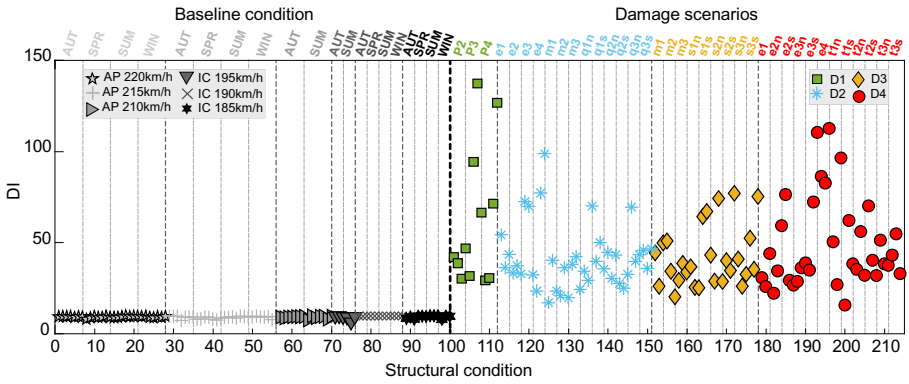

Fig. 18.10 *DI* values obtained with double PCA-based features for all 214 structural conditions considering the responses from all sensors.

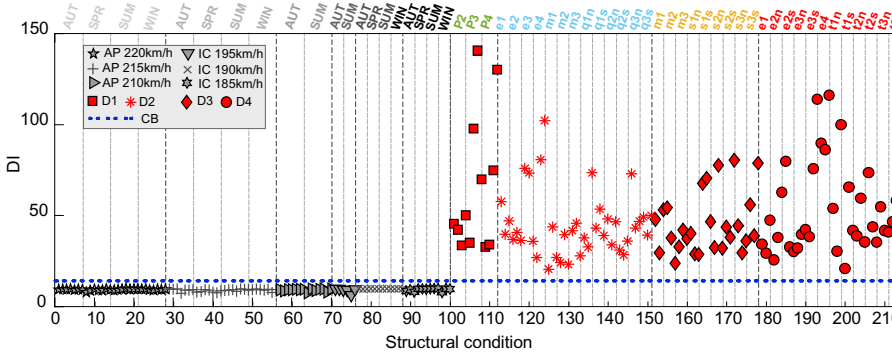

Fig. 18.11 Automatic damage detection using *DI* values for all 214 structural conditions considering the responses from all sensors and a *CB* determined for a significance level of 1%.

where

$$F(x|\,\mu,\sigma) = \frac{1}{\sigma\sqrt{2\pi}} \int_{-\infty}^{x} \mathrm{e}^{-\frac{1}{2}\left(\frac{x-\mu}{\sigma}\right)^2} dy, \quad \text{for } x \in \mathbb{R} \tag{18.6}$$

Thus, a feature is considered an outlier when its *DI* is equal or greater than *CB*. A significance level of 1% was defined, as it is commonly observed in several SHM works addressing damage identification [2,38].

Fig. 18.11 corroborates the effectiveness of the methodology in distinguishing baseline from damage scenarios. The strategy does not display either Type I (false positive) nor Type II errors (false negative).

18.5 Conclusions

This research presents an innovative data-driven SHM strategy for conducting unsupervised damage detection in railway bridge vibration response from traffic-induced excitation, applying multivariate statistical techniques. The strategy consists of fusing sets of acceleration measurements to improve sensitivity and combines:

(i) double PCA for feature extraction and modeling;
(ii) Mahalanobis distance for data fusion;
(iii) outlier analysis for feature discrimination.

The effectiveness of the presented strategy was validated on a bowstring-arch railway bridge through the simulation of several structural conditions using only experimentally obtained actions as input, namely temperature, noise, train loadings, and speeds. Damage severities of 5%, 10%, and 20% stiffness reductions in the concrete slab, diaphragm, and arches were simulated, as well as friction increases in the movements of the bearing.

The damage-sensitive features were extracted by implementing a PCA to the bridge accelerations induced by train crossings in different locations along the bridge.

Statistical parameters were extracted from the principal components to allow data compression. The study of damage-sensitive features obtained from different structural conditions, allowed concluding the supremacy of the environmental and operational variations when compared with damage, proving the importance of feature modeling. Moreover, the information obtained from each feature is different depending on the sensor location and the statistical parameter. PCA was once again implemented to model the features, allowing to successfully remove the environmental and operational effects without losing sensitivity to damage.

To enhance sensitivity, the fusion of the 92 features extracted from all the sensors was implemented and a single damage indicator for each train crossing was defined and obtained. This step proved to be crucial to achieve the highest possible level of information fusion and to obtain a clear distinction between undamaged and damaged conditions.

To automatically detect the presence of damage, an outlier analysis was performed based on a *CB* computed for a significance level of 1%. The robustness and effectiveness of the proposed strategy were demonstrated by automatically detecting the damage scenarios as different from those belonging to undamaged structural conditions. Using features modeled based only on measurements of structural responses, no false detections occurred.

Acknowledgments

This work was financially supported by the Portuguese Foundation for Science and Technology (FCT) through the PhD scholarship SFRH/BD/93201/2013. The authors would like to acknowledge the support of the Portuguese Road and Railway Infrastructure Manager (Infraestruturas de Portugal, I.P), the Portuguese National Laboratory for Civil Engineering (LNEC), the SAFESUSPENSE project—POCI-01-0145-FEDER-031054 (funded by COMPETE2020, POR Lisboa and FCT) and the Base Funding—UIDB/04708/2020 of the CONSTRUCT—Instituto de I&D em Estruturas e Construções—financed by national funds through the FCT/MCTES (PIDDAC). The authors are also sincerely grateful to the European Commission for the financial sponsorship of H2020 MARIE SKŁODOWSKA-CURIE RISE Project, Grant No. 691135 "RISEN: Rail Infrastructure Systems Engineering Network."

References

[1] C.H. Carey, E.J. O'Brien, J. Keenahan, Investigating the use of moving force identification theory in bridge damage detection, Key Eng. Mater. 569–570 (2013) 215–222, https://doi.org/10.4028/www.scientific.net/KEM.569-570.215.

[2] C.R. Farrar, K. Worden, Structural Health Monitoring: A Machine Learning Perspective, Wiley, 2013.

[3] C.R. Farrar, K. Worden, An introduction to structural health monitoring, Philos. Trans. R. Soc. A Math. Phys. Eng. Sci. 365 (1851) (2007) 303–315, https://doi.org/10.1098/rsta.2006.1928.

[4] H. Sohn, C.R. Farrar, F.M. Hemez, D.D. Shunk, D.W. Stinemates, B.R. Nadler, J.J. Czarnecki, A review of structural health monitoring literature: 1996–2001, Los Alamos (USA), 2004.

[5] K. Worden, J.M. Dulieu-Barton, An overview of intelligent fault detection in systems and structures, Int. J. Struct. Health Monit. 3 (1) (2004) 85–98.
[6] C.R. Farrar, S.W. Doebling, D.A. Nix, Vibration-based structural damage identification, Philos. Trans. R. Soc. A Math. Phys. Eng. Sci. 359 (1778) (2001) 131–149, https://doi.org/10.1098/rsta.2000.0717.
[7] A. Yan, G. Kerschen, P. De Boe, J. Golinval, Structural damage diagnosis under varying environmental conditions—part I : a linear analysis, Mech. Syst. Signal Process. 19 (2005) 847–864, https://doi.org/10.1016/j.ymssp.2004.12.002.
[8] A. Alvandi, C. Cremona, Assessment of vibration-based damage identification techniques, J. Sound Vib. 292 (2006) 179–202, https://doi.org/10.1016/j.jsv.2005.07.036.
[9] V. Alves, A. Meixedo, D. Ribeiro, R. Calçada, A. Cury, Evaluation of the performance of different damage indicators in railway bridges, Procedia Eng. 114 (2015) 746–753, https://doi.org/10.1016/j.proeng.2015.08.020.
[10] A. Meixedo, V. Alves, D. Ribeiro, A. Cury, R. Calçada, Damage identification of a railway bridge based on genetic algorithms, in: Maintenance, Monitoring, Safety, Risk and Resilience of Bridges and Bridge Networks—Proceedings of the 8th International Conference on Bridge Maintenance, Safety and Management, IABMAS 2016, Foz Do Iguaçu, Brazil, 2016.
[11] V.N. Alves, M. Oliveira, D. Ribeiro, R. Calçada, A. Cury, Model-based damage identification of railway bridges using genetic algorithms, Eng. Fail. Anal. 118 (August) (2020), https://doi.org/10.1016/j.engfailanal.2020.104845, 104845.
[12] J.P. Santos, C. Crémona, A.D. Orcesi, P. Silveira, Multivariate statistical analysis for early damage detection, Eng. Struct. 56 (2013) 273–285, https://doi.org/10.1016/j.engstruct.2013.05.022.
[13] A. Cury, C. Cremona, Assignment of structural behaviours in long-term monitoring: application to a strengthened railway bridge, Struct. Health Monit. 11 (4) (2012) 422–441, https://doi.org/10.1177/1475921711434858.
[14] D. Posenato, P. Kripakaran, I.F.C. Smith, Methodologies for model-free data interpretation of civil engineering structures, Comput. Struct. 88 (7–8) (2010) 467–482, https://doi.org/10.1016/j.compstruc.2010.01.001.
[15] E. Figueiredo, G. Park, C.R. Farrar, K. Worden, J. Figueiras, Machine learning algorithms for damage detection under operational and environmental variability, Struct. Health Monit. 10 (6) (2010) 559–572, https://doi.org/10.1177/1475921710388971.
[16] O.R. De Lautour, P. Omenzetter, Damage classification and estimation in experimental structures using time series analysis and pattern recognition, Mech. Syst. Signal Process. 24 (2010) 1556–1569, https://doi.org/10.1016/j.ymssp.2009.12.008.
[17] A. Datteo, G. Busca, G. Quattromani, A. Cigada, On the use of AR models for SHM: a global sensitivity and uncertainty analysis framework, Reliab. Eng. Syst. Saf. 170 (2018) 99–115, https://doi.org/10.1016/j.ress.2017.10.017.
[18] R. Azim, M. Gül, Damage detection of steel girder railway bridges utilizing operational vibration response, Struct. Control Health Monit. (2019) 1–15, https://doi.org/10.1002/stc.2447. August.
[19] A. Meixedo, J. Santos, D. Ribeiro, R. Calçada, M. Todd, Damage detection in railway bridges using traffic-induced dynamic responses, Eng. Struct. 238 (2021), https://doi.org/10.1016/j.engstruct.2021.112189, 112189.
[20] A. Meixedo, J. Santos, D. Ribeiro, R. Calçada, M. Todd, Online unsupervised detection of structural changes using train–induced dynamic responses, Mech. Syst. Signal Process. 165 (2022), https://doi.org/10.1016/j.ymssp.2021.108268, 108268.
[21] A. Meixedo, D. Ribeiro, J. Santos, R. Calçada, M. Todd, Real-time unsupervised detection of early damage in railway bridges using traffic-induced responses, Structural Health

Monitoring Based on Data Science Techniques. Structural Integrity, vol. 21, Springer Science and Business Media Deutschland GmbH, 2022, pp. 117–142.
[22] M.I. Friswell, Damage identification using inverse methods, in: Dynamic Methods for Damage Detection in Structures, Springer Wien, New York, 2008.
[23] L. Colombo, C. Sbarufatti, M. Giglio, Definition of a load adaptive baseline by inverse finite element method for structural damage identification, Mech. Syst. Signal Process. 120 (2019) 584–607, https://doi.org/10.1016/j.ymssp.2018.10.041.
[24] S.W. Doebling, C.R. Farrar, M.B. Prime, D.W. Shevitz, Damage identification and health monitoring of structural and mechanical systems from changes in their vibration characteristics: a literature review, Report: LA, 1996.
[25] D. Posenato, F. Lanata, D. Inaudi, I.F.C. Smith, Model-free data interpretation for continuous monitoring of complex structures, Adv. Eng. Inform. 22 (2008) 135–144, https://doi.org/10.1016/j.aei.2007.02.002. 22.
[26] I. Gonzalez, R. Karoumi, BWIM aided damage detection in bridges using machine learning, J. Civ. Struct. Heal. Monit. 5 (5) (2015) 715–725, https://doi.org/10.1007/s13349-015-0137-4.
[27] C. Haynes, M. Todd, Enhanced damage localization for complex structures through statistical modeling and sensor fusion, Mech. Syst. Signal Process. 54–55 (2015) 195–209, https://doi.org/10.1016/j.ymssp.2014.08.015.
[28] W.H. Hu, C. Moutinho, E. Caetano, F. Magalhães, Á. Cunha, Continuous dynamic monitoring of a lively footbridge for serviceability assessment and damage detection, Mech. Syst. Signal Process. (2012), https://doi.org/10.1016/j.ymssp.2012.05.012.
[29] C. Farrar, H. Sohn, K. Worden, Data normalization: a key for structural health monitoring, 2001. Technical Report, Los Alamos National Laboratory; 836(LA-UR-01-4).
[30] F. Cavadas, I.F.C. Smith, J. Figueiras, Damage detection using data-driven methods applied to moving-load responses, Mech. Syst. Signal Process. 39 (1–2) (2013) 409–425, https://doi.org/10.1016/j.ymssp.2013.02.019.
[31] B. Peeters, G. de Roeck, One-year monitoring of the Z24 bridge environmental effects versus damage events, Earthq. Eng. Struct. Dyn. 30 (2) (2001) 149–171.
[32] A. Meixedo, D. Ribeiro, J. Santos, R. Calçada, M. Todd, Progressive numerical model validation of a bowstring-arch railway bridge based on a structural health monitoring system, J. Civ. Struct. Heal. Monit. 11 (2) (2021) 421–449, https://doi.org/10.1007/s13349-020-00461-w.
[33] R. Pimentel, D. Ribeiro, L. Matos, A. Mosleh, R. Calçada, Bridge Weigh-in-Motion system for the identification of train loads using fiber-optic technology, Structures 30 (November 2020) (2021) 1056–1070, https://doi.org/10.1016/j.istruc.2021.01.070.
[34] J. Santos, Smart Structural Health Monitoring Techniques for Novelty Identification in Civil Engineering Structures (PhD Thesis), Instituto Superior Técnico—University of Lisbon, 2014.
[35] D. Ribeiro, J. Leite, A. Meixedo, N. Pinto, R. Calçada, M. Todd, Statistical methodologies for removing the operational effects from the dynamic responses of a high-rise telecommunications tower, Struct. Control Health Monit. 28 (4) (2021), https://doi.org/10.1002/stc.2700, e2700.
[36] W.K. Härdle, L. Simar, Applied Multivariate Statistical Analysis, fourth ed., Springer, 2015.
[37] I.T. Jolliffe, Principal Component Analysis, second ed., Springer, New York, 2002.
[38] J.P. Santos, C. Crémona, L. Calado, P. Silveira, A.D. Orcesi, On-line unsupervised detection of early damage, Struct. Control Health Monit. (2015), https://doi.org/10.1002/stc.